IEEE Access
Multidisciplinary | Rapid Review | Open Access Journal

Received April 20, 2020, accepted May 11, 2020, date of publication May 14, 2020, date of current version May 28, 2020.

Digital Object Identifier 10.1109/ACCESS.2020.2994462

Risk-Averse Home Energy Management System

SAQIB ALI[1], TAHIR NADEEM MALIK[1], AND AAMIR RAZA[2]
[1]Electrical Engineering Department, University of Engineering and Technology Taxila 47080, Pakistan
[2]Islamabad Electric Supply Company, Islamabad 45710, Pakistan

Corresponding author: Saqib Ali (saqib.uet2017@gmail.com)

ABSTRACT Transformation of conventional energy systems into smart grids enables the integration of residential buildings with distributed generations, electro-thermal storages and demand response policies. Further, it improves the household comfort level and helps to preserve the ecological system. Keeping in view the techno-financial impact of residential energy management, optimal handling of residential customers may prove meaningful for peak load reduction, valley filling, and energy conservation. In this regard, this paper devises a residential energy management system (EMS) to optimally schedule appliances, energy sources and electro-thermal storage for reduction of consumption cost and greenhouse (GHG) emissions. Building integrates national grid, natural gas network and solar energy as input carriers, whereas, electricity, heat and cooling as output carriers. To resolve the risk of loss of load, conditional value at risk (CVaR) has been incorporated in the objective function. Comparison demonstrates that under risk-averse approach, energy retaining capability of electric vehicle and thermal energy storage increases by 28.56% and 53.34%, respectively. This stored energy acts as a reserve during absence of solar irradiance and outages on electric and natural gas networks. Moreover, to make EMS more efficient in tracking optimum solutions with faster convergence speed, a hybrid algorithm has been devised by concatenating the modified flower pollination algorithm with mixed-integer linear programming. The proposed algorithm has been validated by comparing its results with the Salp Swarm Algorithm, Grasshopper Optimization Algorithm, Polar Bear Algorithm, Coyote Optimization and Two Cored Flower Pollination Algorithm (FPA). Results manifest that the cost, GHG emissions and execution time drop by 8.98%, 10.81% and 35.064%, respectively.

INDEX TERMS Demand response, energy management, residential buildings, smart grids, stochastic model.

I. INTRODUCTION

Energy systems face problems such as increasing energy prices, energy deficit, network overloading, environmental issues, cybersecurity breach, etc [1]. To resolve these problems, there are multiple options in the conventional grid paradigm such as capacity enhancement of power generation, transmission and distribution infrastructure and renewable energy integration. In contrast, the smart energy grid offers distributed generators (DGs) and demand response (DR) strategies to address these problems [2]. Small scale renewable energy DGs connected to the distribution system may reduce network overloading, generation-demand gap, energy cost, fossil fuel depletion rate and global warming effects due to a decrease in greenhouse gas (GHG) emissions [3].

Among various concepts of smart grid, energy management system (EMS) may play a vital role in decreasing energy consumption cost and emission by optimally dispatching the building components [4]. These components consist of input energy carriers (electricity, natural gas (NG) and solar photovoltaic (PV) power), storages and loads. Customer premises/building represents an energy system node and may be treated as microgrids (μG) [5]. Smart energy distribution system can be considered as a collection of such μGs engaged in bilateral energy trade to benefit both customer and national grid.

Recently, several metaheuristic algorithms have been devised to solve different optimization problems for instance, Salp Swarm Algorithm (Mirjalili 2017) [6], Grasshopper Optimization Algorithm (Saremi 2017) [7], Polar Bear Algorithm (Dawid Połap 2017) [8], Coyote Optimization (Juliano Pierezan and Leandro dos Santos Coelho 2018) [9], and Two Cored Flower Pollination Algorithm (FPA) (Raza 2020) [10]. Devised hybrid modified FPA-Mix-integer linear programming (MILP) algorithm has been compared with these latest algorithms in terms of energy consumption costs, GHG

The associate editor coordinating the review of this manuscript and approving it for publication was Salvatore Favuzza.

emissions, and executions time for the devised energy management control in a residential μG. The literature review of these algorithms are as:

Khan *et al.* developed an energy scheduling technique to optimize the cost and peak to average ratio (PAR) of smart home by using Salp Swarm Algorithm (SSA) [11]. Barik and Das made attempts to achieve the active power management for renewable resources present in isolated μG in MATLAB using SSA [12]. Fathy *et al.* presented an optimal EMS to minimize the total hydrogen consumption and fuel cell (FC) degradation using SSA by considering DER constraints [13]. Rezk *et al.* proposed a novel methodology to minimize the operating cost and network losses of a building using SSA [14]. Sambaiah and Jayabarathi used SSA to optimally allocate distributed energy resources (DERs) and capacitor banks to attain technical, economic, and environmental benefits [15].

Tan *et al.* applied a bio-inspired Grasshopper Optimization Algorithm (GOA) to determine the optimum size of hybrid autonomous μG to maximize the demand-supply reliability and cost minimization [16]. Khitab *et al.* developed an efficient EMS for appliance scheduling in an office building using GOA to reduce PAR, cost, and emissions [17]. Hussain *et al.* proposed a demand-side management strategy to optimally schedule the load units in an industrial building using GOA to minimize cost and PAR and maximize user comfort [18]. Hatata *et al.* proposed a state-of-the-art, precise, consistent and fast under-frequency load management system based on GOA to minimize the load shedding and execution time in addition to maximize the lowest swing frequency [19]. Roy proposed a mathematical optimization framework by hybridization of Particle Swarm Optimization (PSO), Neural Network and GOA to minimize fuel cost, emissions, operating and maintenance costs [20]. Gampa *et al.* proposed a two-stage GOA approach to calculate the optimum size of a diesel engine, shunt capacitor, and EVs charging-discharging station to reduce power factor, voltage deviation, and real power loss. Results showed that performance improvement and convergence time of the proposed GOA were better as compared to PSO and Genetic Algorithm (GA) [21].

Ahmad *et al.* applied Polar Bear Algorithm (PBA) to solve 3, 5, and 6-unit economic dispatch problems including transmission losses and valve point effect to reduce fuel cost and convergence time [22]. Książek *et al.* proposed a technique for a heating plant to maximize its efficiency at the lowest possible cost at different weather conditions using PBA [23].

Al-Dhaifallah *et al.* proposed an optimized EMS to reduce hydrogen consumption, energy cost, emission and maximize the durability of energy sources using a recent and powerful metaheuristic optimization technique known as Coyote Optimization Algorithm (COA) [24]. Chin and Salam applied COA to extract the parameters of single and two diode solar PV cells/modules [25]. Maidl *et al.* applied COA for the optimized operation of a heavy-duty gas turbine to reduce the fuel consumption, emissions under physical constraints. Güvenç and Kaymaz applied COA for the economic dispatch integrated with thermal and wind power generators to reduce cost and convergence time as compared to other metaheuristic techniques [26].

Raza *et al.* proposed a risk-averse two cored energy management system using an energy hub approach to minimize energy cost, emissions and network load variation [10].

In addition to the recent algorithms, many energy management approaches have been adopted in last few years to optimize energy consumption cost and emissions in residential sector.

For example, Hussain *et al.* proposed an efficient home EMS for single as well as multiple homes based on genetic harmony search algorithm to minimize electricity cost, PAR, and maximize user comfort. The optimization problem is solved in MATLAB. The energy cost and PAR are reduced by 46.19%, 56.04% and 38.32%, 50.08% for single and multi-homes, respectively [27] Thomas *et al.* proposed a framework using the MILP-based model for optimal operations of an EMS in a smart building using renewable energy resources (RERs), battery energy storage (BES) system, and plugin electric vehicles (PHEVs) under stochastic and deterministic approaches. The problem was solved using CPLEX optimizer in GAMS [28]. Shareef *et al.* reviewed on HEMS considering residential DR to consider load demand, smart meter, automated load-shedding, scheduling, lighting control, occupancy sensing, remote access, plugin load control and intelligent controllers [29]. Farmani *et al.* devised an EMS for residential μG to deals with deterministic and stochastic cases to minimize the net energy cost [30]. Iqbal *et al.* proposed a grid-connected HEMS for a domestic μG to minimize cost and load deviation along with comfort maximization. The optimization problem was solved using GA, binary PSO, wind-driven optimization (WDO) and grey wolf optimization (GWO) and three new hybrid techniques were proposed by hybridizing GA, binary PSO, WDO and GWO in MATLAB. Results revealed that the proposed techniques reduced energy cost and PAR by 35.02% and 35.60%, respectively [31].

Mehrjerdi and Rakhshani proposed a method to optimally charge-discharge the EVs to eliminate the renewable energy intermittency in a 33 bus IEEE network. The proposed problem was solved in GAMS using non-linear stochastic programming to properly charge and discharge the EVs to avoid degradation [32]. Shakeri *et al.* implemented a HEMS architecture along with a control algorithm to monitor and control the home appliances. The time of use pricing technique was used to minimize the energy consumption cost. Results demonstrated that approximately up to 15% of electricity use was reduced as compared to usual consumption [33]. Nge *et al.* proposed an optimized EMS to maximize the revenue using Lagrange Multipliers by forecasting solar PV generation and the results were compared with the brute-force dynamic programming approach [34]. Ma and Ma proposed an EMS to forecast the power generation as well as load demand using the multi-agent system for a μG. The pro-

posed architecture consisted of three layers, external, prediction and operational layer. The details of the various EMS algorithms were also described [35]. Afrakhte and Bayat proposed a stable and reliable EMS strategy to solve network and economic problems in a μG considering BES and PHEVs. The optimization problem was solved in the targeted search shuffled complex algorithm in MATLAB using a variable weighted multi-objective function. Results demonstrated that the CPU time with the proposed technique decreased significantly as compared with the results solved through GAMS [36].

Seifi *et al.* proposed an EMS for a residential building using grey wolf and shark smell algorithms to converge to the global minima. The simulation was performed in MATLAB. Results showed that cost reduced by 20% and stability increased by 18%, respectively [37]. Chamandoust *et al.* modeled an energy scheduling problem for HEMS to minimize cost, emissions and load deviation. Epsilon-constraint method was used to deal with uncertain behavior of RERs using stochastic approach. Result showed that the cost, emissions and loss of load expectation reduced by 50,034.71 $, 87,220.08 kg and 21.96 MW, respectively [38]. Moghaddam *et al.* proposed an EMS for a residential building to optimally control and monitor RERs and controllable loads using a multi-agent approach. These multiple agents communicated with each other and coordinated with DGs, storages and DR schemes to minimize system operational cost and maximize user comfort [39]. Anvari *et al.* proposed a multi-objective optimization framework for a residential EMS to fulfill the objectives such as energy consumption cost reduction, improve user comfort, optimal schedule home appliances and manage supply-demand gap. Simulations were performed in MATLAB. The μG architecture considered heat and electricity generation sources, load scheduling potentials, heat transfer and thermal dynamics [40]. Monsef *et al.* proposed a thermal-electrical load scheduling model for a residential building to satisfy user comfort and energy cost objectives. Mixed-integer nonlinear programming was used to model RERs, storages and domestic load. The architecture controlled the home appliances and provided a platform for the customers to manage their load profile according to their desires [41]. Sameti and Haghighat proposed a mathematical strategy for the optimal combination of cooling and heating supply chain to save annual cost and emission simultaneously. Mixed-integer linear programming was used to determine the optimal flow and storage using the least-annualized-cost approach in GAMS. Results showed that 67% of emissions reduction was achieved by using the proposed strategy [42]. Sameti and Haghighat identified the net-zero energy district among various optimal solutions to integrate electrical and thermal energy storage using the MILP method in GAMS. The proposed strategy optimized energy generation cost, associated size, used technologies and optimal operating strategy. The best solution for cost and emissions objectives were presented as a set of Pareto optimal solutions [43].

A. CONTRIBUTIONS

Main contributions of this paper are summarized as:

1. Proposed an efficient home energy management system to dispatch building loads, storages and sources.
2. Transformed risk-neutral (without CVaR) control into a risk-averse control.
3. Devised a solution methodology by hybridizing modified FPA and MILP algorithms to track improved results in less amount of time.
4. Compared proposed modified FPA-MILP solution technique with Salp Swarm Algorithm, Grasshopper Algorithm, Polar Bear approach, Coyote Optimization and Two Cored FPA for validation purpose.

The rest of the paper is organized as: in Section-II system architecture and system modeling; in Section-III, proposed solution methodology; in Section-IV, experimental results and case studies; and in Section-V, draw the conclusion.

II. SYSTEM ARCHITECTURE

A. CONCEPTUAL AND IMPLEMENTATION PERSPECTIVE

Fig. 1 shows the layered process of EMS. Building owner accesses EMS control through the first layer termed as user layer by feeding comfort data and appliance preferences. Database layer saves this data and feeds to the optimization layer containing EMS core. Optimization layer generates an optimal dispatch signal to schedule building appliances, energy sources, and storages residing in the service layer. Communication layer acts as a wireless or wired link between optimization and service layers.

Fig. 2 shows the proposed smart home EMS for a residential building. Home EMS unit receives data from customer, weather server and utility server about comfort, irradiance as well as temperature and tariff data, respectively, for generation of optimal dispatch signal. Building contains lights as a curtailable load, iron, washing machine, dryer, dishwasher and pool pump as shiftable appliances, PHEVs,

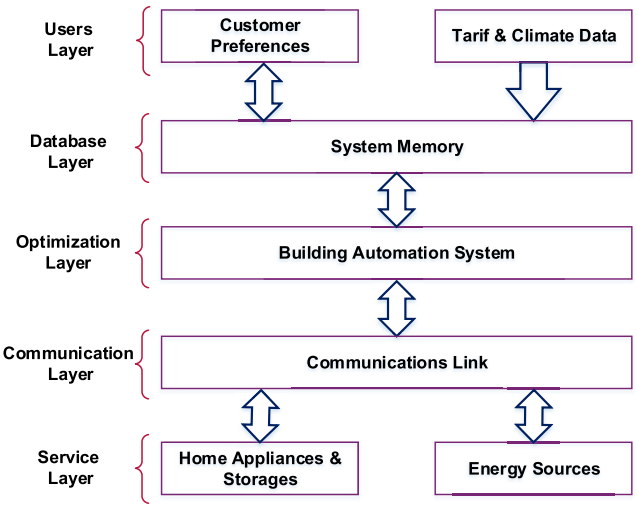

FIGURE 1. Layer process of building energy management control.

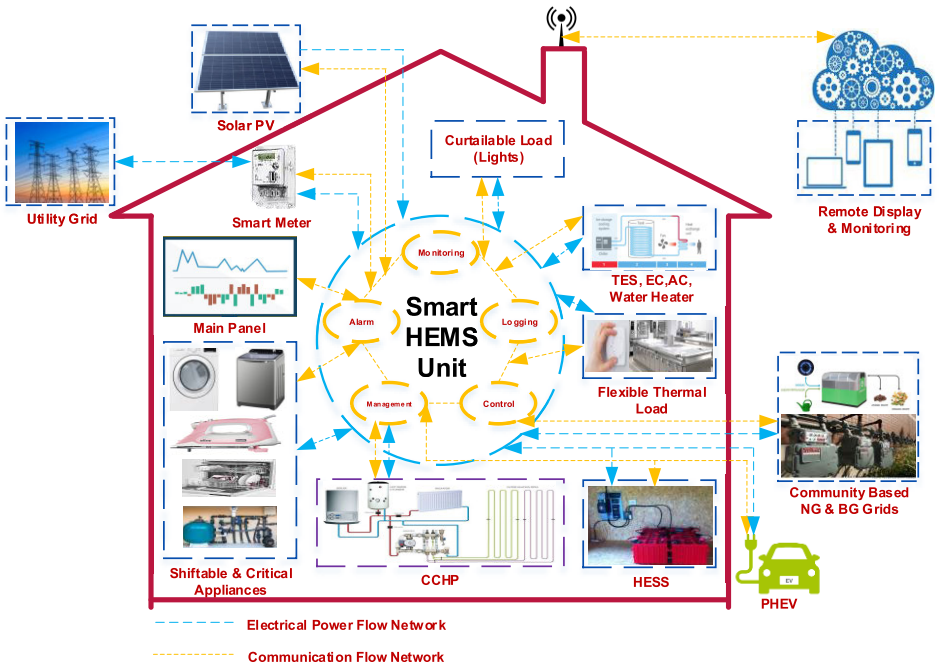

FIGURE 2. Proposed EMS control for residential building.

thermal energy storage, CCHP. Electricity from national grid, NG and solar energy are integrated as input carriers whereas electricity, heat, and cooling are taken as outputs. Energy management system core aims to reduce energy consumption cost and emissions. Further as may be witnessed that EMS communicates with utility and customer for monitoring and control purposes.

B. SYSTEM MODELING

1) BUILDING OWNED GENERATION SOURCES

The building-owned energy generation sources are solar PV panel and combined cooling, heating and power unit (CCHP) units. The models are described below:

a: PHOTOVOLTAIC PANELS

Solar energy proves beneficial for both customer and utility by reducing energy consumption cost and network load, respectively. Moreover, it reduces the threat of global warming effects of fossil fuels. The output power from the solar PV panel installed in the i^{th} home is described as follows [44]:

$$P_{sr,i}(t) = \eta_{sr,i} \cdot S_i \cdot I \cdot (1 - 0.005 \cdot (T_{ext}(t) - 25)) \quad (1)$$

where i, $P_{sr,i}(t)$, $\eta_{sr,i}$, S_i, $I(t)$ and $T_{ext}(t)$ are the number of homes, output power (kW), efficiency of solar cell array (%), array area (m^2), solar irradiance (kW/m^2) and the outdoor temperature (°C), respectively.

For modeling purpose, one year (2013) hourly solar data of Islamabad, Pakistan, is used to calculate the parameters of probability density function of normal distribution. Later on, the Latin hypercube sampling technique [45] was applied to generate 5000 scenarios over 24 hours. To deduce the computational burden, the samples were deduced to 50, using k-means method [46].

Expression for normal distribution is given as below [47]:

$$h(I) = \frac{1}{\sigma\sqrt{2\pi}} e^{\frac{-(1-\mu)^2}{2\sigma^2}} \quad (2)$$

where μ, σ are mean and deviation of normal distribution.

b: COMBINED COOLING AND HEATING POWER SYSTEM

Combined cooling, heating and power unit as tri-generation technology can be used in homes with the ratting of 5 kW or below. Typically, CCHP uses NG and heat is captured with a heat recovery unit (HRU) to use in absorption chiller for room cooling purpose and water heating. Utilization of waste heat increases the energy efficiency of the building. The relationship between the CCHP output power ($P_{chp,i}$) and heat generated ($H_{chp,i}$) is as [44]:

$$H_{chp,i}(t) = P_{chp,i}(t) \cdot \eta_{th,i}/\eta_{e,i} \quad (3)$$

where $\eta_{th,i}$ and $\eta_{e,i}$ are the CCHP thermal as well as electrical efficiencies (%), respectively.

Fuel input ($F_{chp,i}$) and electric power output can be expressed as [44]:

$$F_{chp,i}(t) = P_{chp,i}(t) \cdot \beta/\eta_{e,i} \quad (4)$$

where β is the conversion factor for kWh to m^3, respectively.

The operational constraints on CCHP power (kW) can be expressed as [44]:

$$P^{\min}_{chp,i}(t) \leq P_{chp,i}(t) \leq P^{\max}_{chp,i} \quad (5)$$

where $P^{min}_{chp,i}$ and $P^{max}_{chp,i}$ are minimum and maximum output power (kW) limits, respectively.

The operational constraints on CCHP produced heat is given as [44]:

$$H^{\min}_{chp,i}(t) \leq H_{chp,i}(t) \leq H^{\max}_{chp,i} \tag{6}$$

where $H^{min}_{chp,i}$ and $H^{max}_{chp,i}$ are the minimum and maximum limits on the CCHP produced heat (kWh), respectively.

The ramp rate limits can be expressed as [44]:

$$\left|P_{chp,i}(t) - P_{chp,i}(t-1)\right| \leq ramp_i \tag{7}$$

$$\left|H_{chp,i}(t) - H_{chp,i}(t-1)\right| \leq ramp_i \cdot \eta_{th,i}/\eta_{e,i} \tag{8}$$

where $ramp_i$ is the ramp rate in terms of heat produced.

In actual practice, the fossil fuel supply network such as the NG may or may not be in an outage state. In this paper, the effects of random outages of the NG network on total μG energy consumption cost and the GHG emissions are investigated. Uncertain NG presence is modeled using Monte Carlo simulations. Two generate random network outages, two state Markov Chain process is used [48] in a two-state model, probability density functions representing duration of operation and repair state are assumed to be exponential [49]. Mean time to repair (MTTR) and mean time to failure data (MTTF) is available in ''NERC generator availability data system''.

The conditional probabilities for network availability state are defined as [49]:

$$p\left(\varphi_t = 1 \,|\, \varphi_{t_0} = 1\right) = \frac{\mu_i}{\mu_i + \lambda_i} + \frac{\lambda_i}{\lambda_i + \mu_i} \cdot e^{-(\lambda_i+\mu_i)\cdot(t-t_0)} \tag{9}$$

$$p\left(\varphi_t = 0 \,|\, \varphi_{t_0} = 1\right) = \frac{\lambda_i}{\lambda_i + \mu_i} \cdot (1 - e^{-(\lambda_i+\mu_i)\cdot(t-t_0)}) \tag{10}$$

$$p\left(\varphi_t = 1 \,|\, \varphi_{t_0} = 0\right) = \frac{\mu_i}{\lambda_i + \mu_i} \cdot (1 - e^{-(\lambda_i+\mu_i)\cdot(t-t_0))} \tag{11}$$

$$p\left(\varphi_t = 0 \,|\, \varphi_{t_0} = 0\right) = \frac{\mu_i}{\mu_i + \lambda_i} + \frac{\lambda_i}{\lambda_i + \mu_i} \cdot e^{-(\lambda_i+\mu_i)\cdot(t-t_0)} \tag{12}$$

To represent the presence and absence of the NG network, a series of different states was obtained by putting values of μ_i as MTTR and λ_i as MTTF in above conditional probabilities. t is the current moment and t_o is next moment of time in hours.

The ''0'' represents the unavailability and ''1'' represents the presence of the NG network. To achieve this purpose, 5000 scenarios [49] are generated and reduced to 50. The sum of occurrence probabilities of 50 scenarios is 1.

2) RESPONSIVE LOAD

Responsive load is divided into two categories termed as curtailable loads such as lights and shiftable appliances like washing machine, dryer, iron, pool pump, and dishwasher. All other appliances, such as stoves, TVs, toasters, laptops, ovens, fridges, and computers, are categorized as critical load.

a: SHIFTABLE LOADS

The optimizer shifts appliances from peak to off-peak hours for cost reduction, with required operational time to complete a task. Washing machine, dishwasher, dryer, pool pump, and iron are considered as shiftable loads.. ''Expressions (13-18) represent the appliances' ON/OFF status, the appliance cannot be up and down at the same time, remains OFF outside the customer specified time interval, maximum run hours, minimum up time for the completion of operation and dryer will operate after washing machine ends up, respectively.''

$$up_{i,j}(t) - down_{i,j}(t) = on_{i,j}(t) - on_{i,j}(t-1), \tag{13}$$

$$up_{i,j}(t) - down_{i,j}(t) \leq 1, \quad \forall t \in \left[\alpha_{i,j}, \beta_{i,j}\right] \tag{14}$$

$$\sum_{t \notin T_j} on_{i,j}(t) = 0, \quad \forall t \in T - [\alpha_{i,j}, \beta_{i,j}] \tag{15}$$

$$\sum_{t \in T_j} on_{i,j}(t) = MRH_{i,j}, \quad \forall t \in [\alpha_{i,j}, \beta_{i,j}] \tag{16}$$

$$\sum_{k=t-MUT_j+1}^{t} up^k_{i,j} \leq on_{i,j}(t), \quad \forall t \in \left[\alpha_{i,j}, \beta_{i,j}\right] \tag{17}$$

$$on_{dr}(t) \leq \sum_{k=t-1}^{t-MRH_{wm}} on^k_{wm}(t) \tag{18}$$

where MHR, MUT, $\alpha_{i,j}$, $\beta_{i,j}$, $on_{i,j}(t)$, $up_{i,j}(t)$ and $down_{i,j}(t)$ are maximum run hours, minimum uptime, operation beginning time, operation ending time, ON/OFF state and up and down states of appliances at time t, respectively, for j^{th} appliance of i^{th} building.

b: CURTAILABLE LOAD

Light requirements depend on time. During day time, presence of sunlight reduces appliance generated illumination, however, night hours require increased lighting load. The mathematical model in equation (19) takes external illumination into account to reduce the lighting load. Moreover, curtailment factor has been introduced with a value of 1 in peak hours and 0 in off-peak hours [50].

$$IL_{in,i}(t) + IL_{out}(t) \geq (1 - 0.2 \cdot \rho(t))IL_{req,i}(t) \tag{19}$$

''where $IL_{in,i}(t)$, $\rho(t)$, $IL_{out}(t)$ and $IL_{req}(t)$ are internal/appliance generated illumination (per unit), linear function of electricity price termed as curtailment factor, outer and required illuminations (per unit) at time t, respectively''.

Curtailment factor is equal to 1 during peak and mid-peak hours and 0 in off-peak hours. Required and external illumination data can be found in [28].

c: FLEXIBLE THERMAL LOAD

Heat generated from CCHP is used for room cooling and for water heating. Water temperature is given below [51]:

$$T_{ws,i}(t+1) = [(V_{cold,i}(t) \cdot (T_{cw,i} - T_{ws,i}(t)) + V_i \cdot T_{ws,i}(t)] / V_{i\,ws,i}(t)/(V_i \cdot C_w)] \tag{20}$$

"where $T_{ws,i}(t)$, $V_{cold,i}(t)$, $T_{cw,i}$, V_i and $H_{ws,i}(t)$, C_w are water storage temperature (°C), the volume of entering cold water (liters), temperature of entering cold water (°C), total water storage volume (liters), heat (kWh) injected for water heating at time t and specific heat capacity of water (kWh/°C), respectively".

Room temperature is given as [51]:

$$T_{in,i}(t+1) = T_{in,i}(t) \cdot e^{-1/(R \cdot C_{air})} + [(-R \cdot H_{air,i}(t) + T_{ext}(t)) \times (1 - e^{-1/(R \cdot C_{air})}) \quad (21)$$

"where $T_{in,i}(t)$, $H_{air,i}(t)$, R, and C_{air} are the internal room temperature (°C), heat (kWh) required to maintain air temperature, thermal resistance of building shell (°C/kW), and specific heat capacity of air (kWh/°C), respectively".

Water and room temperature constraints are given below [51]:

$$T_{ws,i}^{\min}(t) \le T_{ws,i}(t) \le T_{ws,i}^{\max} \quad (22)$$

$$T_{in,i}^{\min}(t) \le T_{in,i}(t) \le T_{in,i}^{\max} \quad (23)$$

"where $T_{ws,i}^{min}$, $T_{ws,i}^{max}$, $T_{in,i}^{min}$ and $T_{in,i}^{max}$ are the minimum and maximum water storage as well as room temperatures (°C), respectively".

(IV) PLUG-IN HYBRID ELECTRIC VEHICLE

The PHEV acts as mobile battery storage. It charges in low tariff hours and discharges in peak hours of the electric grid. The presence of PHEVs in bilateral energy transaction mode helps in peak shaving of the network. Equation for PHEV is given as [44]:

$$E_{phev,i}(t+1) = E_{phev,i}(t) + \eta_{G2V,i} \cdot P_{ch,phev,i}(t) \cdot \Delta t - 1/\eta_{V2G,i} \cdot P_{dch,phev,i}(t) \cdot \Delta t \quad (24)$$

"where $E_{phev,i}(t)$, $P_{ch,phev,i}(t)$, $P_{dch,phev,i}$, Δt, $\eta_{G2V,i}$ and $\eta_{V2G,i}$ are energy in the PHEV battery (kWh) at time t, battery charging and discharging power (kW) at time t, duration of charging/discharging (h), grid to vehicle charging efficiency (%) and vehicle to grid discharging efficiency (%), respectively".

PHEV battery charger constraints are as given as [44]:

$$P_{ch,phev,i}(t) \le P_{charger,i}^{\max} \quad (25)$$

$$P_{dch,phev,i}(t) \le P_{charger,i}^{\max} \quad (26)$$

"where $P_{ch,phev,i}(t)$, $P_{dch,phev,i}(t)$ and $P_{charger,i}^{max}$ are battery charging power (kW) at time t and vehicle battery charger rating (kW), respectively".

Upper and lower limits of state of charge [44]:

$$SOC_{phev,min,i} \le SOC_{phev,i}(t) \le SOC_{phev,max,i} \quad (27)$$

"where $SOC_{max,i}$ and $SOC_{min,i}$ are the upper and lower limits on the SOC (%), respectively".

Energy to be stored and available in an electric vehicle is given as [44]:

$$P_{ch,phev,i}(t) \cdot \eta_{G2V,i} \cdot \Delta t \le Cap_i - E_{phev,i}(t) \quad (28)$$

$$P_{dch,phev,i}(t) \cdot 1/\eta_{V2G,i} \cdot \Delta t \le E_{phev,i}(t) \quad (29)$$

"where $P_{ch,phev,i}(t)$, $P_{dch,phev,i}(t)$, Cap_i and $E_{phev,i}(t)$ are vehicle battery charging and discharging power (kW) at time t, capacity of vehicle battery (kW) and energy level in a battery (kWh) at time t, respectively".

3) ELECTRICAL BALANCES

The expression without DR strategies like load shifting, curtailment, and flexible thermal load is described as follows [44]:

$$P_{grid,i}(t) - (P_{ch,phev,i}(t) \cdot \eta_{G2V,i} - P_{dch,phev,i}/\eta_{V2G,i}) + P_{chp,i}(t) + P_{sr,i}(t) = D_{total,i}(t) + (IL_{in,i}(t) \cdot P_{li,i}) + P_{EC,i}(t) \quad (30)$$

"where $P_{grid}(t)$, $D_{total}(t)$, $P_{li,i}$ and $P_{EC}(t)$ are the power fed to or taken from the outer grid (kW), total load (kW), the wattage of lighting load (kW) and power fed to the electric chiller (EC) in (kW) at time t, respectively".

The expression with DR strategies is in shown below [44]:

$$\begin{aligned} &P_{grid,i}(t) - (P_{ch,phev,i}(t) \cdot \eta_{G2V,i} - P_{dch,phev,i}/\eta_{V2G,i}) \\ &\quad + P_{chp,i}(t) + P_{sr,i}(t) \\ &= D_{crit,i}(t) + (IL_{in,i}(t) \cdot P_{li,i}) \\ &\quad + (\sum_{j=1}^{N} O_{i,j}(t) \cdot P_{i,j}) + P_{EC,i}(t) \end{aligned} \quad (31)$$

"where $D_{crit,i}(t)$, $O_{i,j}(t)$ and $P_{i,j}$ are critical load (kW), binary variable representing ON/OFF status of j^{th} shiftable appliance in i^{th} home at time t and wattage of shiftable appliances (kW), respectively."

4) THERMAL BALANCES

The heat balance after CCHP is given as [44]:

$$H_{chp,i} = H_{ws,i} + H_{AC,i} + (-H_{in,i}(t) \cdot \eta_{in,i} + H_{dr,i}/\eta_{dr,i}) \quad (32)$$

"where $H_{chp,i}(t)$, $H_{ws,i}(t)$, $H_{AC,i}(t)$, $H_{in,i}(t)$, $\eta_{in,i}$, $H_{dr,i}(t)$ and $\eta_{dr,i}$ are heat generated by the CCHP (kWh), heat fed to water storage (kWh), heat fed to the AC (kWh), heat injected into the thermal energy storage (TES) (kWh), injection efficiency (%), heat is drawn out of the TES (kWh) and drawing efficiency (%), respectively".

The energy balance for room cooling is given as [44]:

$$H_{AC,i}(t) \cdot COP_{AC,i} + E_{EC,i}(t) \cdot COP_{EC,i} = H_{air,i}(t) \quad (33)$$

"where $COP_{AC,i}$, $E_{EC,i}(t)$, $COP_{EC,i}$ and $H_{air,i}(t)$ are coefficient of performance of the AC (%), electric energy fed to EC (kWh), coefficient of performance of EC (%) and total energy for maintaining air temperature (kWh), respectively".

The ratio of electric energy fed to the EC to total energy for maintaining air temperature is taken as an optimizable feature [44]:

$$Theta_i = E_{EC,i}(t) \cdot COP_{EC,i}/H_{air,i} \quad (34)$$

5) OBJECTIVE FUNCTIONS

The expression for the cost under deterministic and risk-neutral control is given below [44]:

$$Cost_i = min \sum_{t=1}^{24} [P_{grid,i}(t) \cdot PRC_{TOU}(t) + F_{NG,i}(t) \cdot PRC_{NG}(t)] \quad (35)$$

For the risk-averse strategy, CVaR is added to the objective function. The proposed expression for the cost is:

$$Cost_i = \min \left[\omega \cdot \left[\sum_{t=1}^{24} \left[P_{grid,i}(t) \cdot PRC_{TOU}(t) + F_{NG,i}(t) \cdot PRC_{NG}(t) \right] \right] + (1-\omega) \cdot CVAR \right] \quad (36)$$

"where $F_{NG,i}$, $PRC_{NG}(t)$, $P_{net,i}(t)$, PRC_{TOU}, ω and $CVAR$ are the NG (m^3/h) fed to the μG at time t, the NG price (cents), power fed to or taken from the outer grid (kW), time of use (TOU) price of electricity (cents), scaling factor for resilience and conditional value at risk, respectively".

The expression for emissions under deterministic and risk-neutral is given as [44]:

$$Emission_i = min[\sum_{t=1}^{24} [P_{grid,i}(t) \cdot (\mu_{net}^{CO_2} + \mu_{net}^{NO_x} + \mu_{net}^{SO_x}) + F_{chp,i}(t) \cdot \left(\mu_f^{CO_2} + \mu_f^{NO_x} + \mu_f^{SO_x}\right)]] \quad (37)$$

The proposed expression for emission under risk-averse mode is given as:

$$Emission_i = min[\omega[\sum_{t=1}^{24} [P_{grid,i}(t) \cdot (\mu_{net}^{CO_2} + \mu_{net}^{NO_x} + \mu_{net}^{SO_x}) + F_{chp,i}(t) \cdot \left(\mu_f^{CO_2} + \mu_f^{NO_x} + \mu_f^{SO_x}\right)] + (1-\omega).CVAR] \quad (38)$$

"where $\mu_{net}^{CO_2}$, $\mu_{net}^{NO_x}$, $\mu_{net}^{SO_x}$ and $\mu_f^{CO_2}$, $\mu_f^{NO_x}$, $\mu_f^{SO_x}$ are emission rates (kg/h) for grid electricity and gaseous fuel, respectively".

The CVaR can be represented as [39]:

$$CVAR = \alpha + \frac{1}{p \cdot (1-\beta)} \cdot \sum_{s=1}^{p} f(x, y_s) \quad (39)$$

where β is the confidence level, p is the number of scenarios and α is the value at risk.

The linear constrained optimization problem has been solved through MFPA-MILP, using MATLAB ver. R2018a on Pavilion dv6 hp Core i7 laptop with 2.0 GHz processor and 8GB of RAM.

III. PROPOSED SOLUTION METHODOLOGY

Deterministic solution techniques are widely used for problem-solving [10]. These techniques are capable of tracking optimum solution, however, fail with an increase in problem size [52]. On the other hand, evolutionary techniques do not ensure optimum solution and take large execution time, however, successfully solve large-sized complex problems [52]. Authors in [5] compared PSO, cuckoo search, electromagnetism like algorithm, artificial bee colony with FPA and found that it outperforms all others in tracking global solution with less execution time, robustness and rapid convergence [53]. Keeping this in view, FPA may prove an efficient solution strategy for the artificial intelligence-oriented community. To further improve search capability, reduce exe-

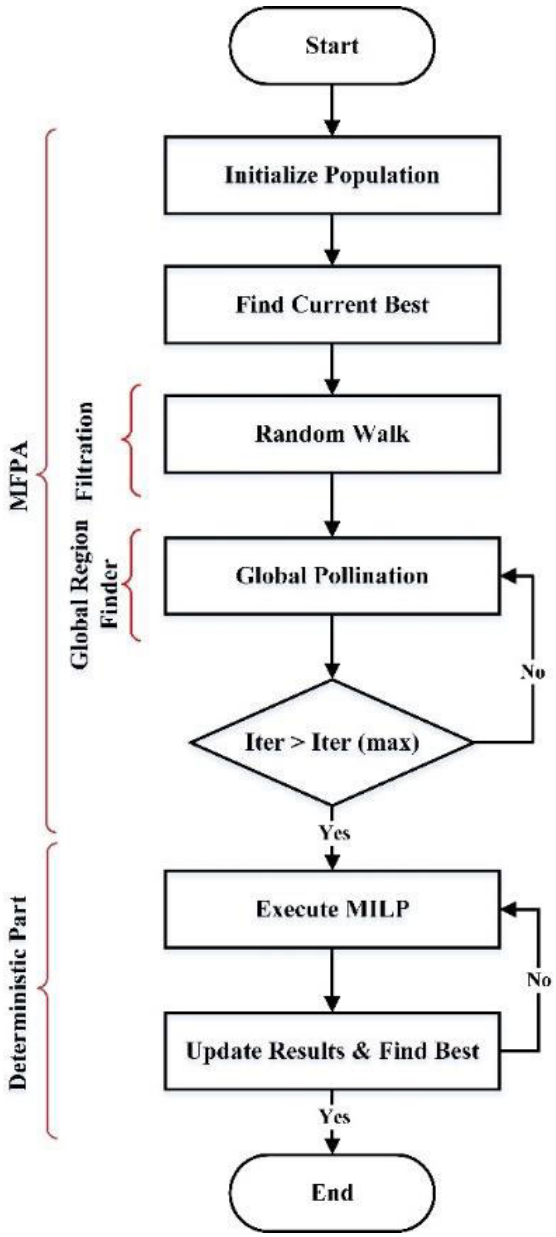

FIGURE 3. Proposed MFPA-MILP algorithm.

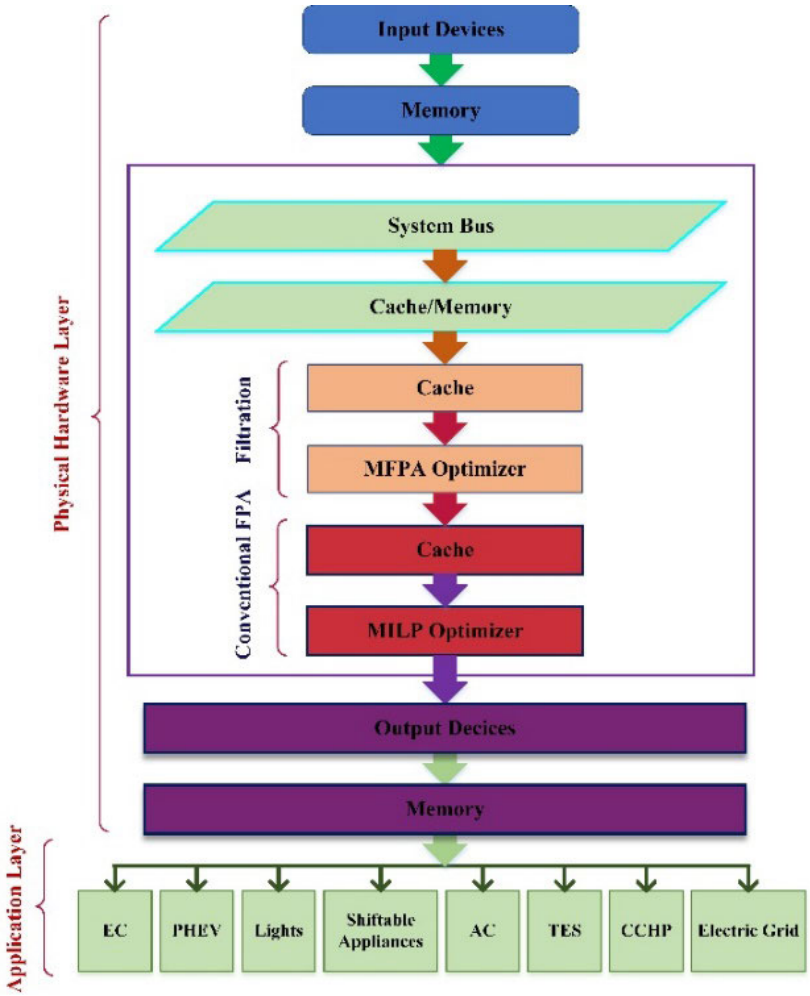

FIGURE 4. Architecture of proposed MFPA-MILP energy management system.

cution time and attain guaranteed global solution, a modified FPA is concatenated with MILP. Proposed modified FPA-MILP is shown in Fig. 3. Modified FPA consists of two sub-layers. First sub-layer acts as a filter and mathematically represented by random walk function. Random walk filters the pollinators and brings it close to the optimum solution. Filtered pollens are injected in second sub-layer termed as global region finder mathematically depicted as global pollination function. This sub-layer divides the search space into multiple regions and selects the one with a global optimum. Second layer termed as deterministic part consists of MILP that locally scans the region containing global optimum. Modified FPA does not contain switching probability that decides between local and global pollination. Moreover, the selected region is scanned locally by MILP instead of the local pollination function. These changes render the proposed solution technique capable of tacking guaranteed optimum solutions in small execution time.

Architectural viewpoint of proposed hybrid EMS is shown in Fig. 4.

Mathematical expressions for operators are provided in this section. Expression of global flight is given as:

$$X_p^{k+1} = X_p^k + \alpha \cdot L(\lambda) \cdot \left(g^* - X_p^k\right) \tag{40}$$

The value of Levy flight size $L(\lambda)$ is:

$$L(\lambda) = \frac{(\lambda \cdot \Gamma(\lambda) \cdot \sin(\lambda))}{\pi \cdot S^{1+\lambda}}, \quad S > 0 \tag{41}$$

Mathematically local pollination can be described as follows:

$$X_p^{k+1} = X_p^k + \alpha \cdot \varepsilon \cdot \left(X_l^m - X_p^k\right) \tag{42}$$

Random walk may be obtained by combining local and global flight expressions as:

$$X_p^{k+1} = X_p^k + w_1 \alpha \cdot L(\lambda) \cdot \left(g^* - X_p^k\right) + \gamma \cdot \varepsilon \cdot w_2 \cdot \left(X_l^m - X_m^k\right) \tag{43}$$

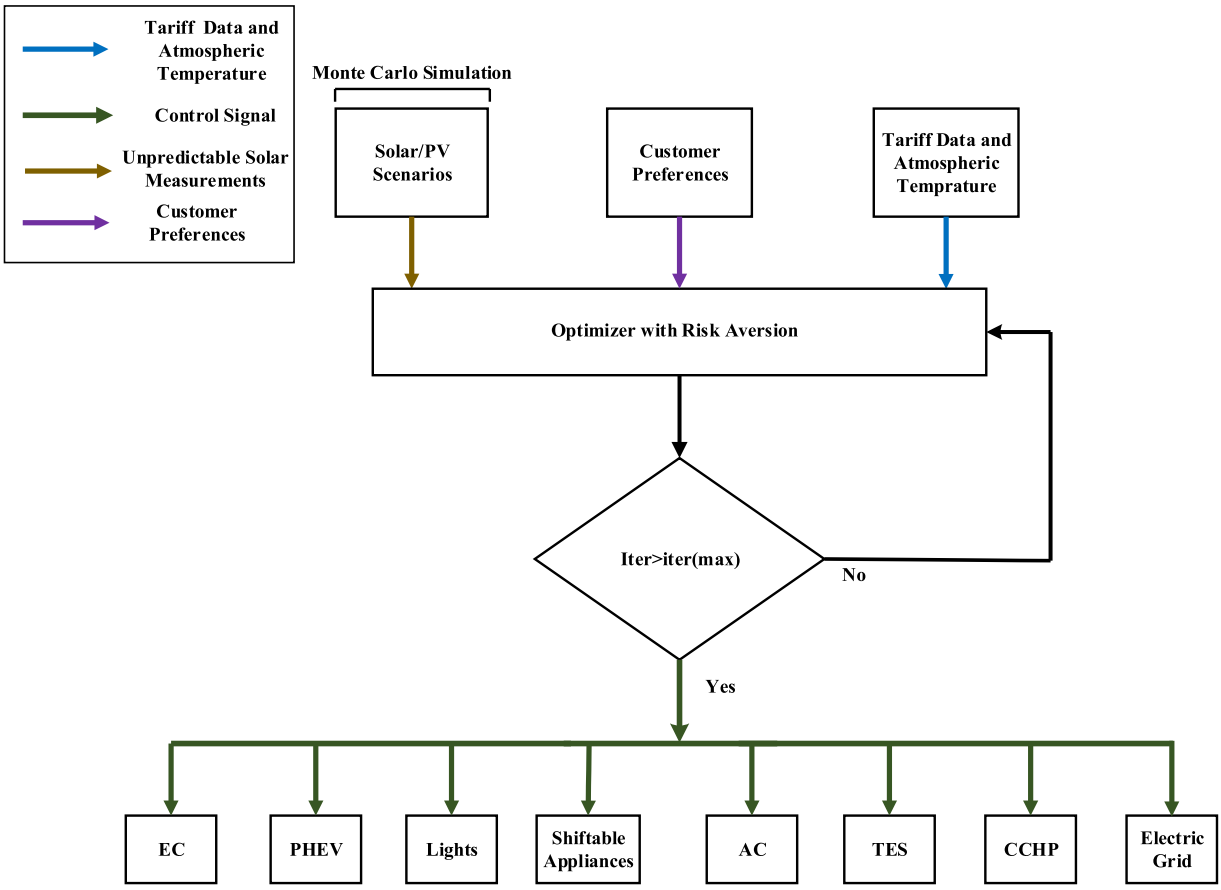

FIGURE 5. Flowchart of complete study of the proposed method.

TABLE 1. The main parameters' setting of algorithms.

Algorithm	Parameters
Hybrid MFPA-MILP	n = 50, switch probability P = 0.8, γ 1 = 1, γ2 = 3, for Levy flight, λ = 1.5, cloning array = [9, 8, 7, 6, 5, 4 , 3, 2, 1, 1, 1, 1, 1, 1]
FPA	n = 50, switch probability P = 0.8, γ = 0.01, for Levy flight λ = 1.5
BAT	n = 50, Loudness=0.5, pulse rate =0.5, minimum frequency=0, maximum frequency = 2
FF	n = 50, Randomness value (alpha=0.25), minimum value attractiveness of a firefly (beta = 0.2), Absorption coefficient (gamma = 1), γ = 0.01, for Levy flight λ = 1.5
GA	n = 50, Cross over=0.8, mutation function is Gaussian with values: Scale =1 and Shrink=1
SA	Annealing function: Fast annealing, Reannealing interval = 100, Initial temperature =100

TABLE 2. Comparison of optimal function values [52].

Algorithm	f_{min}	f_{max}	Mean	Standard deviation
Hybrid MFPA-MILP	**0**	**0**	**0**	**0**
FPA	0	3.193e-12	1.698e-13	5.898e-13
Modified FPA	0	0	0	0
BAT	5.981e-10	9.949	2.023	2.224
Fire fly	3.646e-10	3.307e-08	9.212e-09	7.458e-09
GA	4.014e-13	0.994	0.0663	0.252
Simulated annealing	3.82e-08	1.989	0.657	0.749

where w_1 and w_2 are scalar dynamic adaptive weights. These weights are defined as follows:

$$w_1 = w_1^{max} - itter \cdot \frac{w_1^{max} - w_1^{min}}{itter_{max}} \tag{44}$$

$$w_2 = \frac{\min[F\ (itter)\ , F_{avg}]}{\max[F\ (itter)\ , F_{avg}]} \tag{45}$$

Flow chart of the complete study is given in Fig. 5. Optimizer receives all input parameters to optimally dispatch all sources, storage, and appliances.

TABLE 3. MILP-MFPA parameters.

Parameters	Values
Number of iterations	500
Search agents	100
Lambda (λ)	1.5
Alpha (α)	0.1
Random number (ε)	[0,1]
Scaling factors	0.1

A. VALIDATION OF PROPOSED HYBRID MFPA-MILP

Proposed solution technique is validated using Rastrigin's function as it is multi-model with poor explorative capability. Function is evaluated using rang $[-6.18, +6.18]$. Mathematical expression of this function is taken from [52]. The parameter setting of proposed algorithm and other five algorithms are illustrated in Table 1. Comparison of results has been shown in Table 2. Result shows that proposed hybrid MFPA-MILP algorithm outperforms, compared to FPA, modifies FPA, BAT algorithm, firefly algorithm, GA and Simulated annealing.

IV. RESULTS AND CASE STUDIES

In order to test the performance of MFPA-MILP, it is applied to the proposed framework. In addition to this, the performance of MFPA-MILP is compared with the following meta-heuristic algorithms: Salp Swarm Algorithm, Grasshopper Algorithm, Polar Bear Algorithm, Coyote Optimization, and Two Cored FPA. The parameter settings of MFPA-MILP can be seen in Table 3, the number of search agents is set to 100 and the maximum number of iterations is set to 500. For other controlling parameters of each algorithm, the values in the latest version [8]–[10], [54], [55] are used to ensure the best performance and tabulated in Table 1. The parameters of appliances, sources, load, solar irradiance data, and tariff data are taken from ref [10].

Table 4 discusses case studies. Case-1 considers existing state of power system with customer turning ON/OFF appliances at his/her own choice and without curtailment in lighting load. This case does not take DR policies and TES into account. Temperature of room and water is controlled by heat led control. Under such thermal control, water and room temperatures are strictly maintained at 70 °C and 22 °C. In case-2, DR programs like load shifting flexible thermal

TABLE 4. Case studies.

Case Studies	Dumb charging	DR Program			TES	Smart PHEV
		Load shifting	Load curtailment	Flexible thermal load		
Case-1	✓					
Case-2	✓	✓	✓	✓		
Case-3		✓	✓	✓	✓	✓
Case-4		✓	✓	✓	✓	✓

TABLE 5. Comparison of case studies using MFPA-MILP.

Case Studies	Homes	Energy Cost	CCHP (kW)	Purchased Power (kW)	Sold Power (kW)	Revenue	Emission
Case-1	1	162.124	16.845	22.814	11.872	152.221	-
	2	134.458	15.267	17.958	11.971	154.145	-
Case-2	1	134.254	17.847	22.875	17.125	217.256	-
	2	103.245	16.612	19.257	18.048	226.267	-
Case-3	1	91.240	21.146	16.803	19.015	245.758	-
	2	99.925	19.879	16.957	18.466	232.941	-
Case-4	1	101.257	-	16.147	11.264	-	16.581
	2	109.127	-	14.875	10.269	-	15.334

TABLE 6. Base Case studies from conventional FPA.

Case Studies	Homes	Energy Cost	CCHP (kW)	Purchased Power (kW)	Sold Power (kW)	Revenue	Emission
Case-1	1	173.6645	15.2616	24.7180	10.5187	133.5881	-
	2	146.5546	13.8566	19.4375	10.4907	133.2314	-
Case-2	1	146.5428	16.3492	24.4491	15.3851	195.3904	-
	2	112.7386	15.2612	21.0320	16.0218	203.4773	-
Case-3	1	102.3040	19.8939	18.6703	17.9010	227.3423	-
	2	111.3966	18.4290	18.1511	16.0766	211.7294	-
Case-4	1	111.2448	-	17.6234	9.8564	-	18.3457
	2	120.4086	-	16.6467	8.9599	-	17.1919

TABLE 7. Comparison of MFPA-MILP with Conventional FPA algorithm for 30 runs.

Case Studies	Home	Iteration Count	Algorithm	Max. Execution Time (sec)	Min. Execution Time (sec)	Avg. Execution Time (sec)	S.D	Var.	Percentage Reduction (%)
Case-4	1	500	Conventional FPA	15.421	11.342	14.519	0.442	0.195	35.064
			Hybrid MFPA-MILP	13.316	7.108	9.428	0.491	0.241	

TABLE 8. Comparison of MFPA-MILP with other recent metaheuristic optimization techniques.

Case Studies	Homes	SSA		GOA		PBOA		COA		TC-FPA		MFPA-MILP	
		Cost	Emission	Cost	Emission	Cost	Emission	Cost	Emission	Cost	Emission	Cost	Emission
Case-1	1	172.32	-	174.12	-	199.89	-	187.11	-	168.25	-	162.12	-
	2	142.84	-	144.97	-	180.23	-	161.18	-	141.75	-	134.45	-
Case-2	1	143.36	-	144.10	-	168.55	-	158.12	-	142.87	-	134.25	-
	2	111.82	-	112.11	-	165.87	-	128.98	-	111.16	-	103.24	-
Case-3	1	98.842	-	99.042	-	127.10	-	113.58	-	98.314	-	91.240	-
	2	108.21	-	110.41	-	139.24	-	121.42	-	107.12	-	99.925	-
Case-4	1	109.77	17.246	110.03	19.357	147.125	29.872	131.13	22.754	108.51	17.249	101.25	16.581
	2	118.31	16.481	119.21	16.481	128.22	27.231	122.35	21.319	117.27	16.481	109.12	15.334

load, load curtailment and dumb charging are considered. Energy management system control shifts dishwasher, dryer, washing machine, pool pump and iron from peak to off peak hours for energy cost reduction. Flexible thermal load control in contrast to heat led control allows the room and water temperature to vary between customer specified windows. The water and room temperature variation limits are 60 °C to 80 °C and 21 °C to 25 °C. Moreover, lighting load curtails by 20% during peak and mid-peak hours. In case-3 smart PHEV and TES are incorporated. In smart operational mode PHEV charges from 12 am to 8 am during off peak hours to 6.68 kW, goes out from 8 am till 4 pm. As PHEV arrives back home, it discharges in the building from 4 pm till 12 am. Case-4 considered all the attributes of case-3 and considered both cost and emission simultaneously.

A. SIMULATION RESULTS UNDER DETERMINISTIC CONDITIONS

As may be observed in Table 5 that in case-1, the output of CCHP unit reduces, consequently lowering revenue and

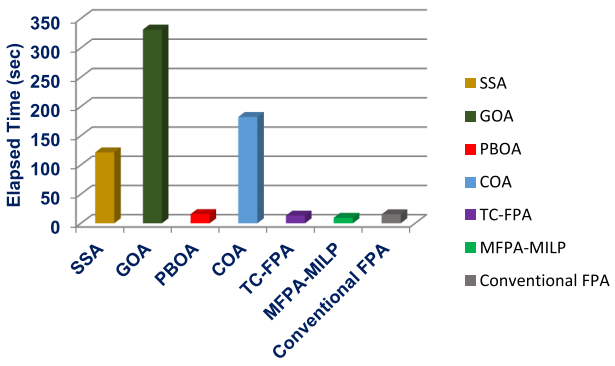

FIGURE 6. Case-4, Home-1: Elapsed time using conventional FPA and MFPA-MILP with recent metaheuristic techniques.

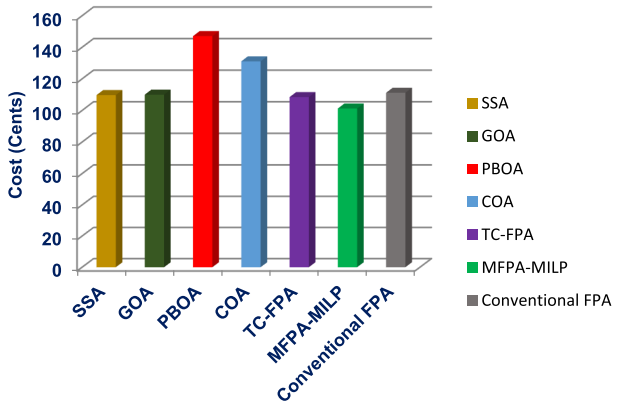

FIGURE 7. Case-4, Home-1: Comparison of cost using conventional FPA and MFPA-MILP with recent metaheuristic techniques.

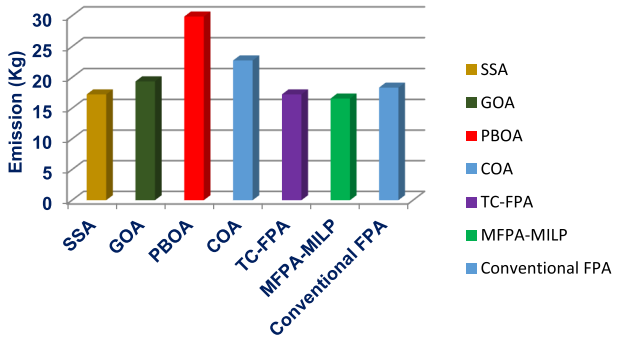

FIGURE 8. Case-4, Home-1: Comparison of emission using conventional FPA, MFPA-MILP and recent metaheuristic techniques.

power sold. Such dynamics occur due to sharp temperature control. This case shows that due to fine control of temperature, the cost rises with a decrease in revenue. Moreover, the absence of DR scheme plays an important role in rise in energy cost. Another noteworthy point is that cost of home-

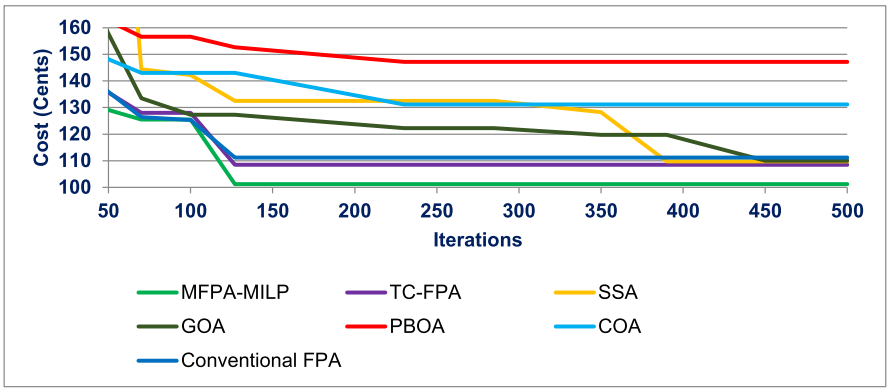

FIGURE 9. Case-4, Home-1: Convergence curve using conventional FPA and MFPA-MILP with recent metaheuristic techniques.

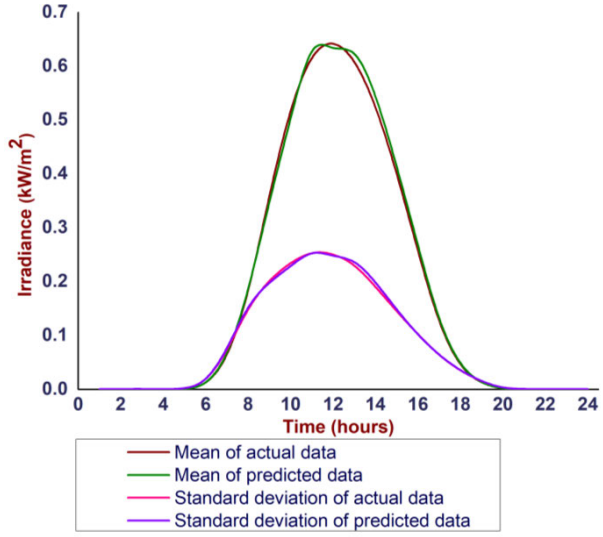

FIGURE 10. Mean as well as SD of actual and predicted data.

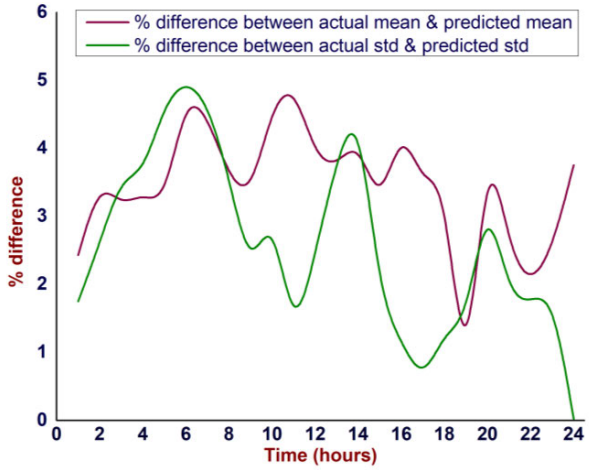

FIGURE 11. Percentage difference among actual and predicted means as well as standard deviation.

1 is high with low revenue compared to home-2, due to dumb presence of PHEV in the former building.

Case-2 takes into account DR programs like load shifting flexible thermal load, load curtailment and dumb charging are considered. Allowed range for temperature variation is 60 °C to 80 °C and 21 °C to 25 °C for water and room, respectively. Table 5 shows that CCHP output increases compared to case-1 with the reduction in cost and increase in power sold and revenue. Increase in CCHP output and sold power is due to the inclusion of flexible thermal load. Allowed temperature fluctuation enables CCHP unit to generate more power. Cost reduction is due to load shifting and curtailment in the lighting load.

Case-3 incorporates TES and smart PHEV. It includes TES in both buildings and intelligent PHEV in home-1. Table 5 shows that cost reduces compared to cases 1 and 2. Moreover, reduction in power purchase, increase in revenue, sold power and output of CCHP are observed. Results show that presence of smart electrical and thermal energy storage serves customer interest.

Case-4 takes all the attributes of case-3 addressing energy cost and emission minimization using Pareto front sets [56]. This case addresses both energy cost and emission by considering environmental concerns. Table 5 shows a decrease in power purchase for reduced emissions. This decrease is due to high emission rate of energy purchase from national grid than for energy generated from NG. Likewise, sold power also reduces.

B. COMPARISON OF CONVENTIONAL FPA AND PROPOSED MILP-MFPA WITH RECENT METAHEURISTIC ALGORITHMS

Comparison of proposed MFPA-MILP (results are shown in Table 5) is provided with conventional FPA. Results of conventional FPA are provided in Table 6 [10]. Comparison shows that the proposed algorithm is capable of tacking global optimum better than conventional FPA in all four cases cost reduces. Table 7 displays that proposed algorithm exe-

TABLE 9. Comparison of case studies using MFPA-MILP under solar uncertainties with risk-neutral control, scenario 5.

Case Studies	Homes	Energy Cost	CCHP (kW)	Purchased Power (kW)	Sold Power (kW)	Revenue	Emission
Case-1	1	180.186	17.221	23.715	10.513	134.512	-
	2	151.748	15.847	19.205	10.264	133.455	-
Case-2	1	150.248	18.325	24.425	15.954	201.615	-
	2	118.478	17.124	20.814	16.842	207.617	-
Case-3	1	102.556	21.721	18.142	17.152	229.581	-
	2	114.287	20.146	18.426	16.245	218.135	-
Case-4	1	116.348	-	17.548	9.865	-	18.124
	2	120.248	-	16.428	8.561	-	17.441

TABLE 10. Comparison of case studies using MFPA-MILP under solar uncertainties with risk-neutral control, scenario 10.

Case Studies	Homes	Energy Cost	CCHP (kW)	Purchased Power (kW)	Sold Power (kW)	Revenue	Emission
Case-1	1	148.325	15.578	20.329	12.991	161.458	-
	2	121.137	14.319	15.729	13.156	171.983	-
Case-2	1	117.598	16.125	20.249	18.689	238.226	-
	2	87.415	14.834	19.257	19.510	247.667	-
Case-3	1	77.267	19.657	14.287	20.219	263.548	-
	2	76.157	17.497	14.319	19.897	249.351	-
Case-4	1	88.328	-	14.497	13.356	-	14.712
	2	91.246	-	12.948	11.782	-	13.897

TABLE 11. Comparison of case studies using MFPA-MILP under solar uncertainties with risk-averse control, scenario 5.

Case Studies	Homes	Energy Cost	CCHP (kW)	Purchased Power (kW)	Sold Power (kW)	Revenue	Emission
Case-1	1	184.348	16.957	23.602	10.834	134.497	-
	2	156.548	15.716	19.325	10.378	133.133	-
Case-2	1	155.814	18.612	24.124	15.649	201.297	-
	2	121.812	16.995	20.325	16.625	207.899	-
Case-3	1	106.012	21.634	18.622	17.425	229.248	-
	2	119.364	20.223	18.514	16.451	218.913	-
Case-4	1	121.533	-	17.325	9.695	-	17.992
	2	124.214	-	16.816	8.941	-	17.654

cutes 35.064% faster than conventional FPA. Such improvement on speed makes EMS core to react rapidly against ever effectively changing weather and load conditions. For further validation of proposed technique comparison has been provided with recently invented metaheuristic algorithms such as Salp Swarm Algorithm (SSA), Grasshopper (GOA), Polar Bear (PBOA), Coyote Optimization Algorithm (COA), and Two Cored FPA (TC-FPA). Results are shown in Table 8 proving the improved global optimum tacking capability of the devised algorithm. Fig. 6 shows the elapsed time using conventional FPA and MFPA-MILP with recent metaheuristic techniques. Fig. 7 shows the comparison analysis (case-4, home-1) of the cost calculated from conventional FPA and proposed MILP-MFPA with other recent metaheuristic algorithms. Comparison of emission (case-4, home-1) calculated from conventional FPA and proposed algorithm with a recent algorithm can be seen in Fig. 8.

Fig. 9 shows the convergence curves of case-4, home 1, using conventional FPA and proposed MFPA-MILP algorithm with recent metaheuristic techniques. Proposed algorithm converges in fewer iterations than all others provided in the figure.

C. SIMULATION RESULTS UNDER UNCERTAIN SOLAR IRRADIANCE WITH RISK NEUTRAL CONTROL

In this subsection, 5000 random solar irradiance scenarios are generated and reduced to 50. Among 50 scenarios, 5^{th} (with the lowest occurrence probability of 0.923%) and 10^{th} (with the highest occurrence probability of 60%) are selected for validation purposes. Another worth consideration aspect is that simple performing Monte Carlo simulation for the generation of solar irradiation values at each time steps may result in unrealistic scenarios. Therefore, validation of predicted solar irradiance values is required. Predicted data having a

TABLE 12. Comparison of energy cost and emission for home 1 at confidence level 0.90 for case 4 under scenario 5 with MFPA-MILP algorithm.

Hours	Policy		% Increase	Policy		% Increase
	Risk neutral SOC	Risk-averse SOC		Risk neutral TES	Risk-averse TES	
1	0.418	0.477	14.11	1.255	1.903	51.6
2	0.51	0.614	20.39	-0.875	-0.954	9.0
3	0.87	0.773	11.15	-1.635	-1.958	19.8
4	0.771	1	29.70	0	0	0
5	0.99	1	1.01	0	0	0
6	1	1	0.00	1.369	1.991	45.4
7	1	1	0.00	0.95	1.1	15.8
8	1	1	0.00	0	0	0
9	0.843	1	18.62	0.841	1.301	54.7
10	0.742	0.903	21.70	-0.2	-0.419	109.5
11	0.639	0.901	41.00	0.857	1.445	68.6
12	0.591	0.86	45.52	0	0	0
13	0.581	0.81	39.41	0.501	0.811	61.9
14	0.541	0.799	47.69	0	0	0
15	0.469	0.718	53.09	0	0	0
16	0.461	0.767	66.38	0	0	0
17	0.435	0.768	76.55	0.333	0.341	2.4
18	0.434	0.749	72.58	0	0	0
18	0.401	0.699	74.31	1.258	1.618	28.6
20	0.321	0.678	111.21	1.501	2.211	47.3
21	0.291	0.591	103.09	-1	-1.59	59.0
22	0.287	0.459	59.93	0.07	0.315	350.0
23	0.301	0.344	14.29	0.529	0.708	33.8
24	0.3	0.341	13.67	0	0	0
Average	0.592	0.760	+28.56	0.240	0.368	+53.34
Cost	120.248	124.214	+3.298	-	-	-
Emission	17.441	17.654	+1.22	-	-	-

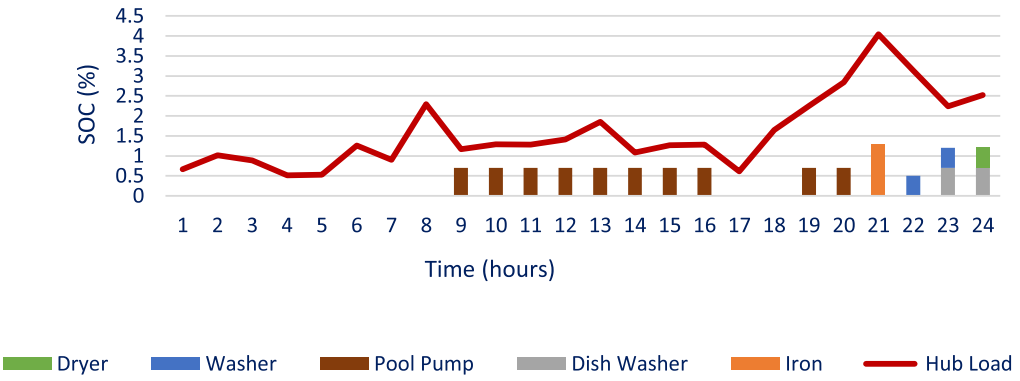

FIGURE 12. Case 4, Home 1: Building load after DR with uncertain solar irradiance.

dimension of 5000 × 24 was derived from actual data with dimensions of 365 × 24 for the year 2013, Islamabad, Pakistan. Mean and standard deviation computed on an hourly basis for actual and predicted matrices are as shown in Fig. 10. Moreover, the percentage difference between actual and predicted data regarding their means and standard deviations was computed and shown in Fig. 11. The deviation between actual and predicted data for each hour is not more than 5%, which validates that the predicted values are close to reality.

Results after the application of scenario 5 are presented in Table 9. As devised control does not contain CVaR in the objective function, therefore, it is termed as risk-neutral. Case studies in Table 9 show that cost in all four cases increases compared to Table 5 due to the reduction of solar power from 15.88 kW (under deterministic conditions) to

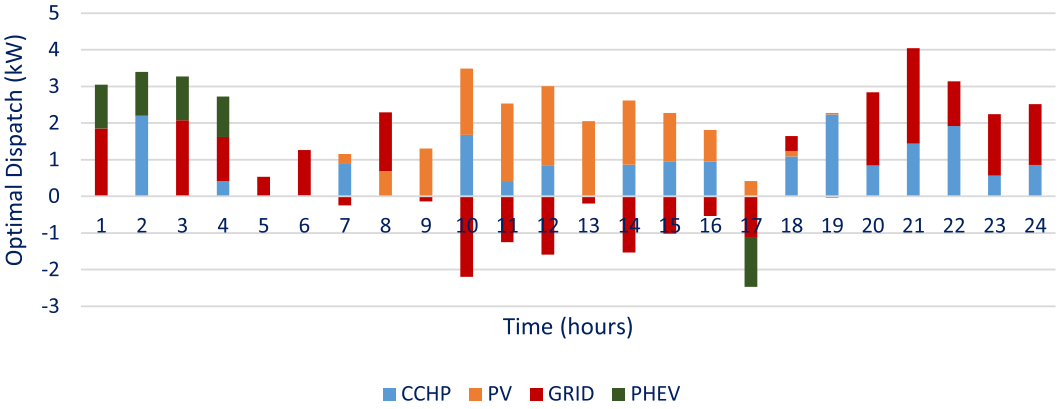

FIGURE 13. Case 4, Home 1: Optimal electrical dispatch with uncertain solar irradiance.

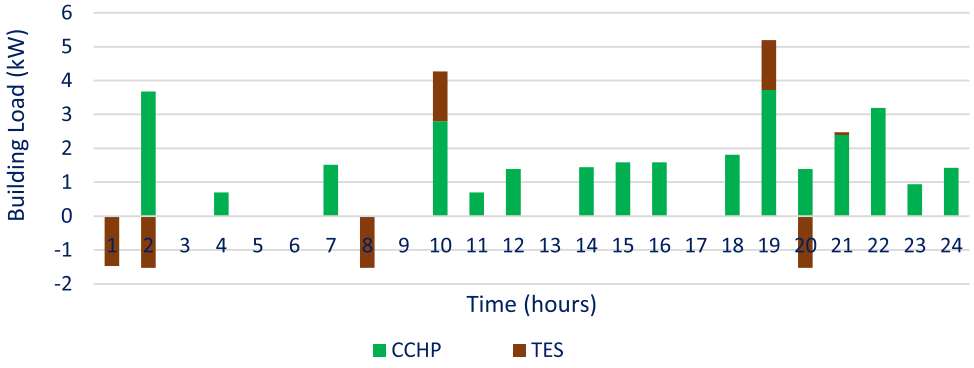

FIGURE 14. Case 4, Home 1: Optimal thermal dispatch with uncertain solar irradiance.

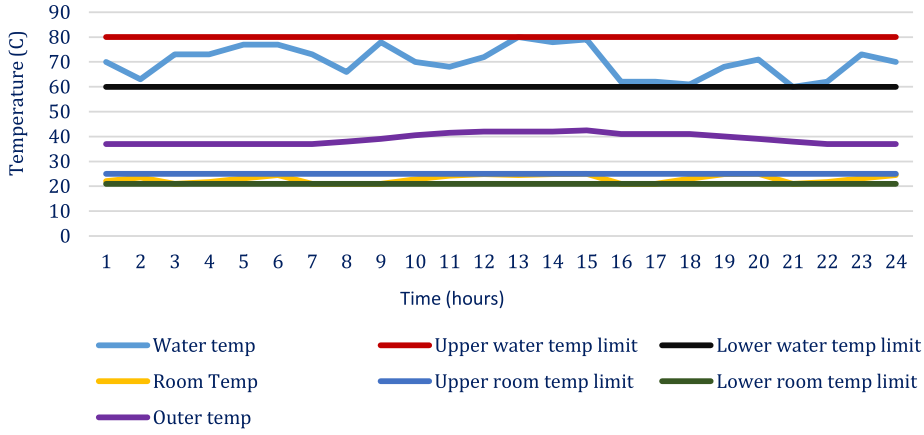

FIGURE 15. Case 4, Home 1: Water and room temperatures with uncertain solar irradiance.

12.62 kW (under stochastic conditions). Likewise, CCHP output and purchasing power increase. However, sold power and revenue decrease. Application of scenario 10 shows that due to increasing in solar power from 15.88 kW to 17.93 kW, the cost, purchased power and CCHP output decrease with a rise in sold power and revenue as can be seen in Table 10.

D. SIMULATION RESULTS UNDER UNCERTAIN SOLAR IRRADIANCE WITH RISK AVERSE CONTROL

Reduction in solar energy in scenario 5 (Table-IX) resulted in an increase in cost on one hand and may result in loss of load on the other hand. Due to this, some parts of the building load may remain unserved. To overcome this issue of loss of load, CVaR is added in the objective function for risk aversion.

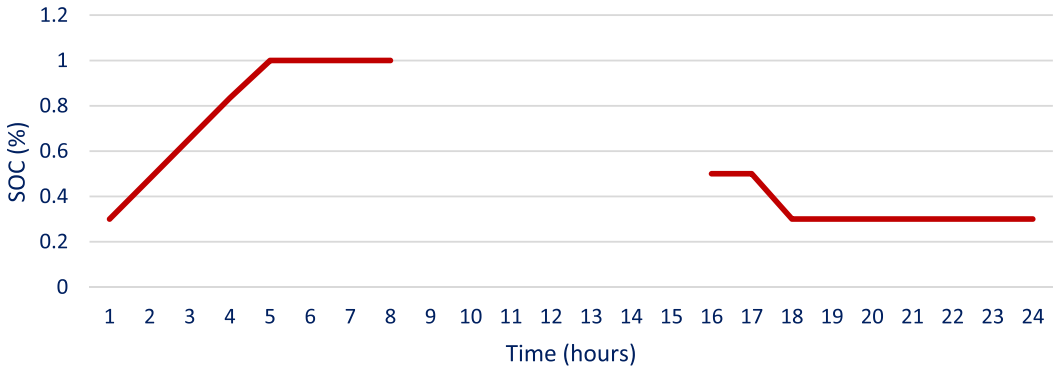

FIGURE 16. Case 4, Home 1: State of charge with uncertain solar irradiance.

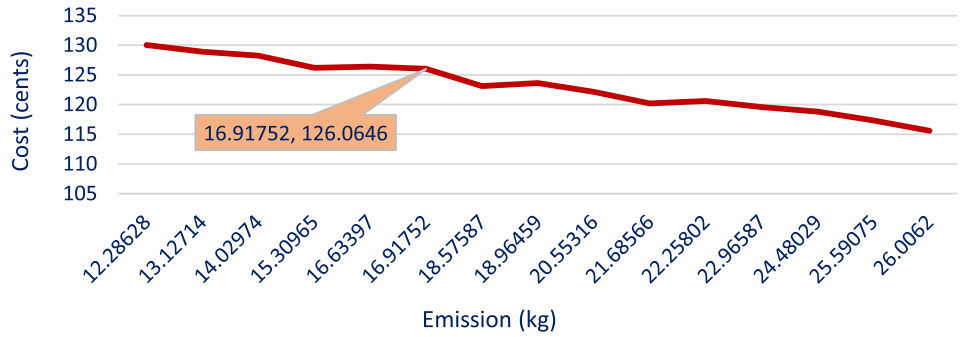

FIGURE 17. Case 4, Home 1: Pareto optimal sets with uncertain solar irradiance.

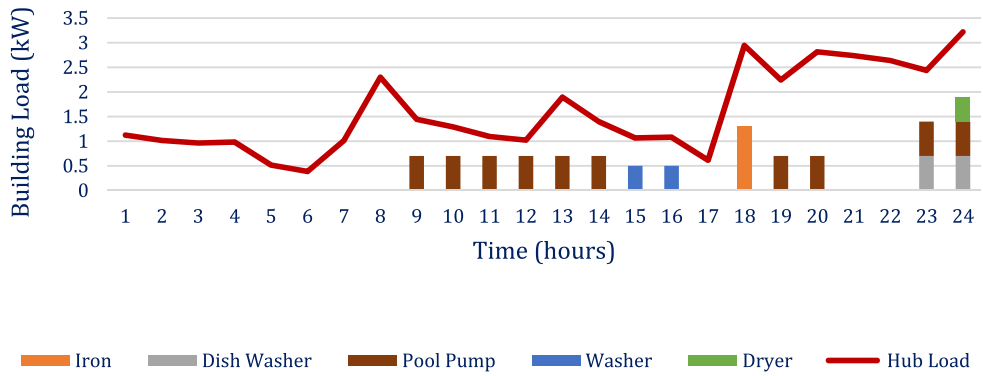

FIGURE 18. Case 4, Home 2: Building load with uncertain solar irradiance.

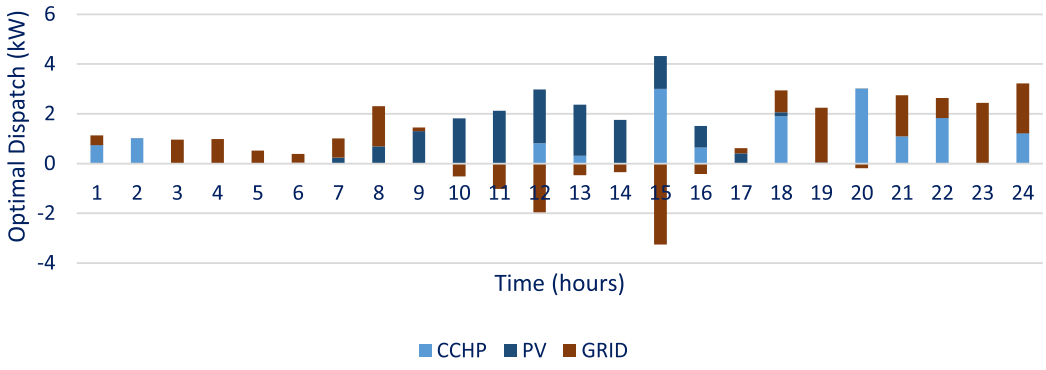

FIGURE 19. Case 4, Home 2: Optimal electric dispatch with uncertain solar irradiance.

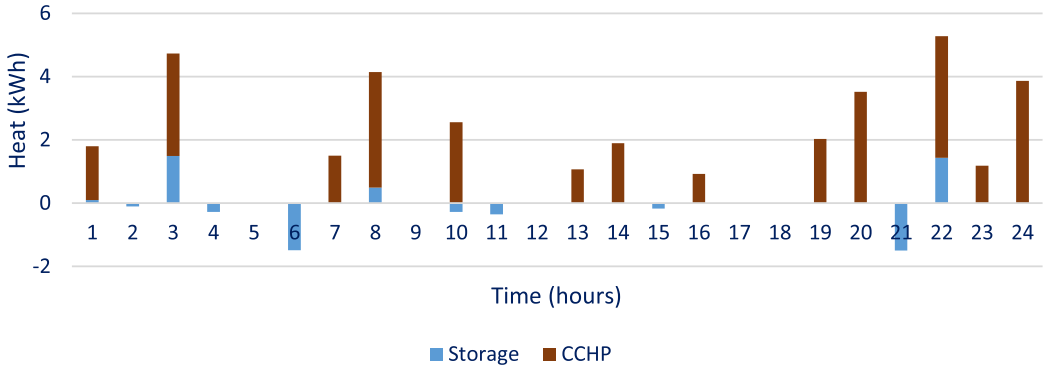

FIGURE 20. Case 4, Home 2: Optimal thermal dispatch with uncertain solar irradiance.

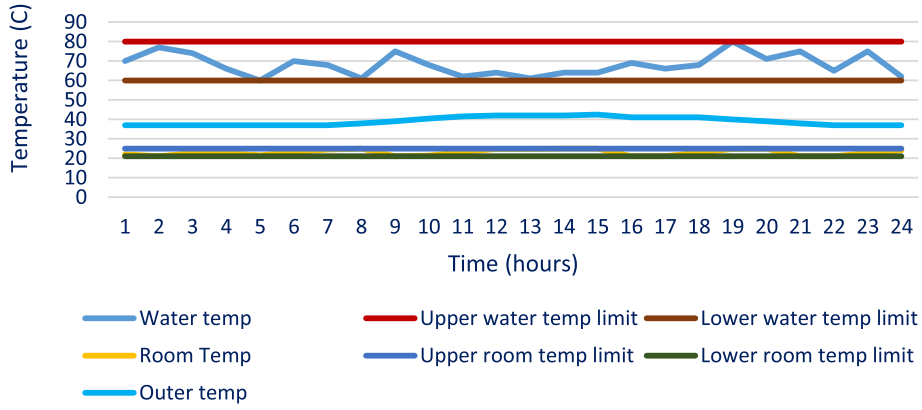

FIGURE 21. Case 4, Home 2: Water and room temperatures with uncertain solar irradiance.

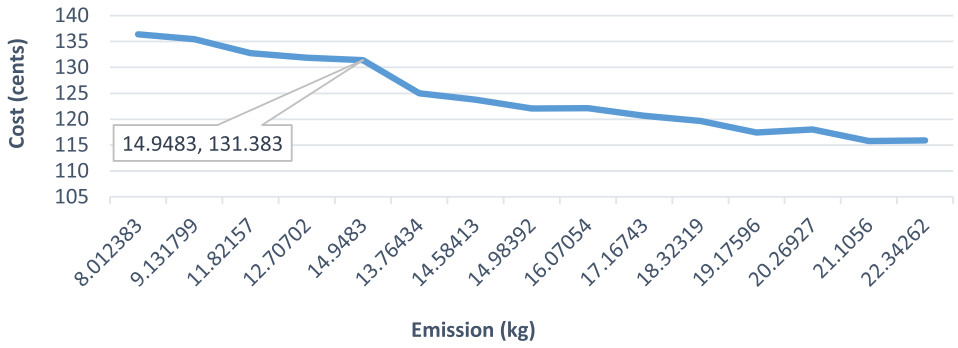

FIGURE 22. Case 4, Home 2: Pareto optimal sets with uncertain solar irradiance.

Results under scenario 5 with risk aversion characteristics are shown in Table 11. As may be witnessed that by the addition of CVaR, the cost in all cases increases a bit in comparison to the cost in Table 9. However, Table 12 compares the energy storage in PHEV and TES under the risk-neutral and risk-averse modes. As may be observed that although cost in risk-averse mode increases, the energy retaining capability of PHEV and TES increases compared to that in risk-neutral mode by 28.56% and 53.34%, respectively for confidence level 0.90. This stored energy serves as a reliable reserve during the hours of low solar irradiance or carrier outages to avoid loss of load.

Fig.s 12-17 show building load, optimal electrical dispatch, optimal thermal dispatch, water and room temperatures, state of charge and Pareto optimal sets with uncertain solar irradiance for case-4, home-1. Similarly, Fig.s 18-22 show building load, optimal electrical dispatch, optimal thermal dispatch, water, and room temperatures and Pareto optimal sets with uncertain solar irradiance for case-4, home-2.

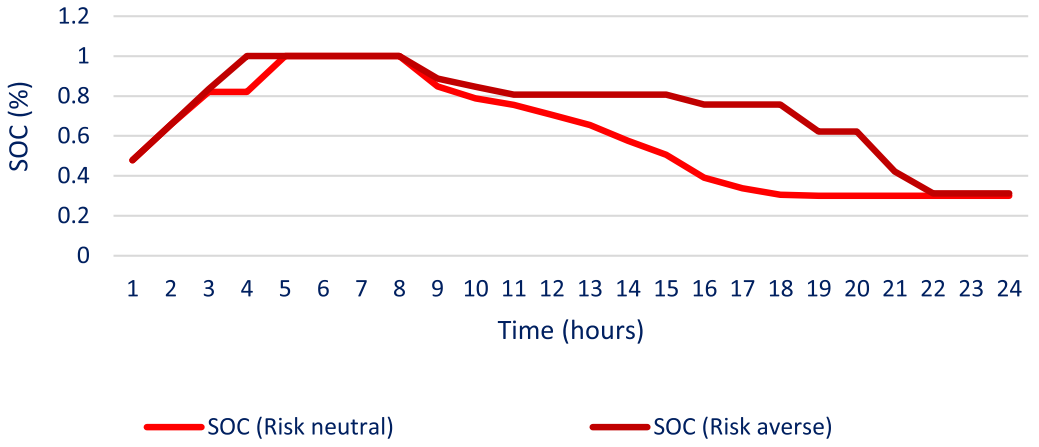

FIGURE 23. Case 4, Home 1: Optimal EV presence with uncertain solar at confidence level 0.90.

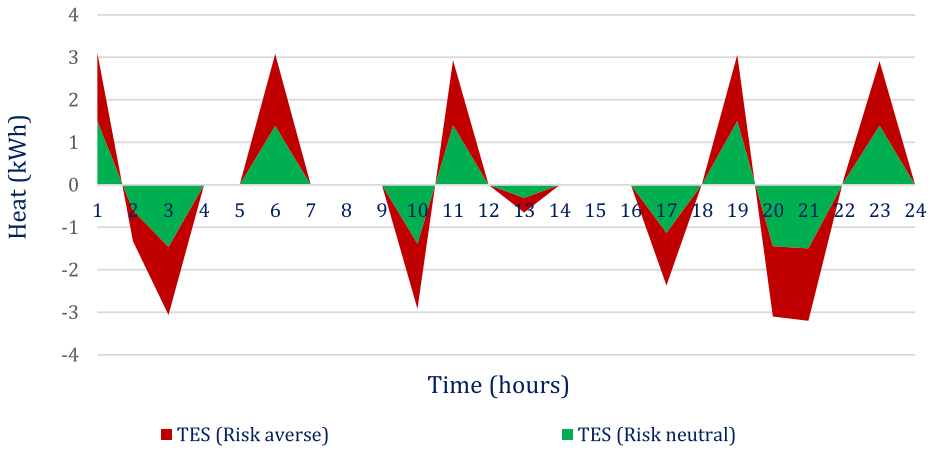

FIGURE 24. Case 4, Home 1: Optimal TES at confidence level 0.90.

Figs. 23-24 show that energy stored in PHEV battery and TES under risk-averse mode is greater than the risk-neutral mode.

V. CONCLUSIONS

This paper devises building energy management modules to reduce energy costs and emissions. Residential building contains CCHP, solar PV panel, electric chiller, absorption chiller, PHEV, shiftable load, curtailable load, and critical demand. Combined cooling and heating power plant generated heat is used for room cooling and water hearing purpose. Case 1 represents the existing state of the power system. Case 2 includes DR programs such as shiftable load, curtailable load, and flexible thermal load. In response to this, results show that energy cost reduces. Case 3 includes smart PHEV and thermal energy storage. Inclusion of energy storage reduces cost, purchased power, emission along with a rise in CCHP output power and revenue. Case 4 is bi-objective simultaneously reducing energy cost and emission. Building EMS is first solved under deterministic conditions. However, later on, solved with the stochastic presence of solar irradiance. Simulation under probabilistic solar irradiance shows that energy cost and emission depend on the occurrence probability of suitable or unsuitable scenarios. To overcome the loss of load against low solar energy during bad weather, CVAR is added to the objective function. The inclusion of CVAR increases cost a bit with improved energy retaining capability of PHEV and TES. To devise an improved algorithm with better tracking speed, improved efficiency and capability to reach global optimum, MILP and modified FPA are concatenated together. Results prove that the proposed algorithm proves superior to Salp Swarm Algorithm, Grasshopper Algorithm, Polar Bear Algorithm, Coyote Optimization and Two Cored FPA. Future work intends to propose building connected to a central district heating system for bidirectional flow of heat.

REFERENCES

[1] T. Ayodele, A. Jimoh, J. Munda, and J. Agee, "Challenges of grid integration of wind power on power system grid integrity: A review," *World*, vol. 3, pp. 618–626, Aug. 2020.

[2] Y. Wang, Y. Huang, Y. Wang, M. Zeng, F. Li, Y. Wang, and Y. Zhang, "Energy management of smart micro-grid with response loads and distributed generation considering demand response," *J. Cleaner Prod.*, vol. 197, pp. 1069–1083, Oct. 2018.

[3] S. Mhanna, A. C. Chapman, and G. Verbic, "A fast distributed algorithm for large-scale demand response aggregation," *IEEE Trans. Smart Grid*, vol. 7, no. 4, pp. 2094–2107, Jul. 2016.

[4] M. M. Iqbal, M. I. A. Sajjad, S. Amin, S. S. Haroon, R. Liaqat, M. F. N. Khan, M. Waseem, and M. A. Shah, "Optimal scheduling of residential home appliances by considering energy storage and stochastically modelled photovoltaics in a grid exchange environment using hybrid grey wolf genetic algorithm optimizer," *Appl. Sci.*, vol. 9, no. 23, p. 5226, 2019.

[5] A. Raza and T. N. Malik, "Energy management in commercial building microgrids," *J. Renew. Sustain. Energy*, vol. 11, no. 1, Jan. 2019, Art. no. 015502.

[6] H. Faris, S. Mirjalili, I. Aljarah, M. Mafarja, and A. A. Heidari, "Salp Swarm algorithm: Theory, literature review, and application in extreme learning machines," in *Nature-Inspired Optimizers*. Cham, Switzerland: Springer, 2020, pp. 185–199.

[7] H. Hichem, M. Elkamel, M. Rafik, M. T. Mesaaoud, and C. Ouahiba, "A new binary grasshopper optimization algorithm for feature selection problem," *J. King Saud Univ. Comput. Inf. Sci.*, vol. 102, Nov. 2019.

[8] D. Połap, "Polar bear optimization algorithm: Meta-heuristic with fast population movement and dynamic birth and death mechanism," *Symmetry*, vol. 9, no. 10, p. 203, 2017.

[9] J. Pierezan and L. Dos S. Coelho, "Coyote optimization algorithm: A new Metaheuristic for global optimization problems," in *Proc. IEEE Congr. Evol. Comput. (CEC)*, Jul. 2018, pp. 1–8.

[10] A. Raza, T. N. Malik, M. F. N. Khan, and S. Ali, "Energy management in residential buildings using energy hub approach," in *Building Simulation*. Beijing, China: Tsinghua Univ. Press, 2020, pp. 363–386.

[11] S. Khan, Z. A. Khan, N. Javaid, S. M. Shuja, M. Abdullah, and A. Chand, "Energy efficient scheduling of smart home," in *Proc. Workshops Int. Conf. Adv. Inf. Netw. Appl.* Cham, Switzerland: Springer, 2019, pp. 67–79.

[12] A. K. Barik and D. C. Das, "Active power management of isolated renewable microgrid generating power from Rooftop solar arrays, sewage waters and solid urban wastes of a smart city using Salp Swarm algorithm," in *Proc. Technol. Smart-City Energy Secur. Power (ICSESP)*, Mar. 2018, pp. 1–6.

[13] A. Fathy, H. Rezk, and A. M. Nassef, "Robust hydrogen-consumption-minimization strategy based Salp Swarm algorithm for energy management of fuel cell/supercapacitor/batteries in highly fluctuated load condition," *Renew. Energy*, vol. 139, pp. 147–160, Aug. 2019.

[14] M. Tolba, H. Rezk, A. A. Z. Diab, and M. Al-Dhaifallah, "A novel robust methodology based Salp Swarm algorithm for allocation and capacity of renewable distributed generators on distribution grids," *Energies*, vol. 11, no. 10, p. 2556, 2018.

[15] K. S. Sambaiah and T. Jayabarathi, "Optimal allocation of renewable distributed generation and capacitor banks in distribution systems using Salp Swarm algorithm," *Int. J. Renew Energy Res.*, vol. 9, no. 9, pp. 96–107, Mar. 2019.

[16] A. L. Bukar, C. W. Tan, and K. Y. Lau, "Optimal sizing of an autonomous photovoltaic/wind/battery/diesel generator microgrid using grasshopper optimization algorithm," *Sol. Energy*, vol. 188, pp. 685–696, Aug. 2019.

[17] I. Ullah, Z. Khitab, M. Khan, and S. Hussain, "An efficient energy management in office using bio-inspired energy optimization algorithms," *Processes*, vol. 7, no. 3, p. 142, 2019.

[18] I. Ullah, I. Hussain, and M. Singh, "Exploiting grasshopper and cuckoo search bio-inspired optimization algorithms for industrial energy management system: Smart industries," *Electronics*, vol. 9, no. 1, p. 105, 2020.

[19] M. Talaat, A. Y. Hatata, A. S. Alsayyari, and A. Alblawi, "A smart load management system based on the grasshopper optimization algorithm using the under-frequency load shedding approach," *Energy*, vol. 190, Jan. 2020, Art. no. 116423.

[20] K. Roy, "Analysis of power management and cost minimization in MG—A hybrid GOAPSNN technique," *Int. J. Numer. Model., Electron. Netw., Devices Fields*, vol. 32, no. 5, p. e2624, 2019.

[21] S. R. Gampa, K. Jasthi, P. Goli, D. Das, and R. C. Bansal, "Grasshopper optimization algorithm based two stage fuzzy multiobjective approach for optimum sizing and placement of distributed generations, shunt capacitors and electric vehicle charging stations," *J. Energy Storage*, vol. 27, Feb. 2020, Art. no. 101117.

[22] S. Fayyaz, A. Ahmad, and M. I. Babar, "Solution of economic dispatch problem using polar bear optimization algorithm," *J. Fundam. Appl. Sci.*, vol. 11, no. 2, pp. 562–577, 2019.

[23] M. Woźniak, K. Książek, J. Marciniec, and D. Połap, "Heat production optimization using bio-inspired algorithms," *Eng. Appl. Artif. Intell.*, vol. 76, pp. 185–201, Nov. 2018.

[24] A. Fathy, M. Al-Dhaifallah, and H. Rezk, "Recent coyote algorithm-based energy management strategy for enhancing fuel economy of hybrid FC/Battery/SC system," *IEEE Access*, vol. 7, pp. 179409–179419, 2019.

[25] V. J. Chin and Z. Salam, "Coyote optimization algorithm for the parameter extraction of photovoltaic cells," *Sol. Energy*, vol. 194, pp. 656–670, Dec. 2019.

[26] J. Pierezan, G. Maidl, E. M. Yamao, L. Dos Santos Coelho, and V. C. Mariani, "Cultural coyote optimization algorithm applied to a heavy duty gas turbine operation," *Energy Convers. Manage.*, vol. 199, Nov. 2019, Art. no. 111932.

[27] H. Hussain, N. Javaid, S. Iqbal, Q. Hasan, K. Aurangzeb, and M. Alhussein, "An efficient demand side management system with a new optimized home energy management controller in smart grid," *Energies*, vol. 11, no. 1, p. 190, 2018.

[28] D. Thomas, O. Deblecker, and C. S. Ioakimidis, "Optimal operation of an energy management system for a grid-connected smart building considering photovoltaics' uncertainty and stochastic electric vehicles' driving schedule," *Appl. Energy*, vol. 210, pp. 1188–1206, Jan. 2018.

[29] H. Shareef, M. S. Ahmed, A. Mohamed, and E. Al Hassan, "Review on home energy management system considering demand responses, smart technologies, and intelligent controllers," *IEEE Access*, vol. 6, pp. 24498–24509, 2018.

[30] F. Farmani, M. Parvizimosaed, H. Monsef, and A. Rahimi-Kian, "A conceptual model of a smart energy management system for a residential building equipped with CCHP system," *Int. J. Electr. Power Energy Syst.*, vol. 95, pp. 523–536, Feb. 2018.

[31] Z. Iqbal, N. Javaid, S. Iqbal, S. Aslam, Z. Khan, W. Abdul, A. Almogren, and A. Alamri, "A domestic microgrid with optimized home energy management system," *Energies*, vol. 11, no. 4, p. 1002, 2018.

[32] H. Mehrjerdi and E. Rakhshani, "Vehicle-to-grid technology for cost reduction and uncertainty management integrated with solar power," *J. Cleaner Prod.*, vol. 229, pp. 463–469, Aug. 2019.

[33] M. Shakeri, M. Shayestegan, S. M. S. Reza, I. Yahya, B. Bais, M. Akhtaruzzaman, K. Sopian, and N. Amin, "Implementation of a novel home energy management system (HEMS) architecture with solar photovoltaic system as supplementary source," *Renew. Energy*, vol. 125, pp. 108–120, Sep. 2018.

[34] C. L. Nge, I. U. Ranaweera, O.-M. Midtgård, and L. Norum, "A real-time energy management system for smart grid integrated photovoltaic generation with battery storage," *Renew. Energy*, vol. 130, pp. 774–785, Jan. 2019.

[35] J. Ma and X. Ma, "A review of forecasting algorithms and energy management strategies for microgrids," *Syst. Sci. Control Eng.*, vol. 6, no. 1, pp. 237–248, Jan. 2018.

[36] H. Afrakhte and P. Bayat, "A contingency based energy management strategy for multi-microgrids considering battery energy storage systems and electric vehicles," *J. Energy Storage*, vol. 27, Feb. 2020, Art. no. 101087.

[37] A. Seifi, M. H. Moradi, M. Abedini, and A. Jahangiri, "An optimal programming among renewable energy resources and storage devices for responsive load integration in residential applications using hybrid of grey wolf and shark smell algorithms," *J. Energy Storage*, vol. 27, Feb. 2020, Art. no. 101126.

[38] H. Chamandoust, G. Derakhshan, S. M. Hakimi, and S. Bahramara, "Tri-objective scheduling of residential smart electrical distribution grids with optimal joint of responsive loads with renewable energy sources," *J. Energy Storage*, vol. 27, Feb. 2020, Art. no. 101112.

[39] A. Anvari-Moghaddam, A. Rahimi-Kian, M. S. Mirian, and J. M. Guerrero, "A multi-agent based energy management solution for integrated buildings and microgrid system," *Appl. Energy*, vol. 203, pp. 41–56, Oct. 2017.

[40] A. Anvari-Moghaddam, J. M. Guerrero, J. C. Vasquez, H. Monsef, and A. Rahimi-Kian, "Efficient energy management for a grid-tied residential microgrid," *IET Gener., Transmiss. Distrib.*, vol. 11, no. 11, pp. 2752–2761, Aug. 2017.

[41] A. Anvari-Moghaddam, H. Monsef, and A. Rahimi-Kian, "Cost-effective and comfort-aware residential energy management under different pricing schemes and weather conditions," *Energy Buildings*, vol. 86, pp. 782–793, Jan. 2015.

[42] M. Sameti and F. Haghighat, "Hybrid solar and heat-driven district cooling system: Optimal integration and control strategy," *Sol. Energy*, vol. 183, pp. 260–275, May 2019.
[43] M. Sameti and F. Haghighat, "Integration of distributed energy storage into net-zero energy district systems: Optimum design and operation," *Energy*, vol. 153, pp. 575–591, Jun. 2018.
[44] A. Raza and T. N. Malik, "Biogas supported bi-level macro energy hub management system for residential customers," *J. Renew. Sustain. Energy*, vol. 10, no. 2, Mar. 2018, Art. no. 025501.
[45] D. Cai, D. Shi, and J. Chen, "Probabilistic load flow computation using copula and latin hypercube sampling," *IET Gener., Transmiss. Distrib.*, vol. 8, no. 9, pp. 1539–1549, Sep. 2014.
[46] S. A. Korkmaz and F. Esmeray, "Quality lignite coal detection with discrete wavelet transform, discrete Fourier transform, and ANN based on k-means clustering method," in *Proc. 6th Int. Symp. Digit. Forensic Secur. (ISDFS)*, Mar. 2018, pp. 1–6.
[47] E. S. Watson, "Applications of incomplete gamma functions to the incomplete normal distribution," Open Access J. Ltd, Visakhapatnam, India, Tech. Rep., 2015, vol. 1, no. 1.
[48] Y. Zhao, A. Fatehi, and B. Huang, "A data-driven hybrid ARX and Markov chain modeling approach to process identification with time-varying time delays," *IEEE Trans. Ind. Electron.*, vol. 64, no. 5, pp. 4226–4236, May 2017.
[49] X. Zhang, M. Shahidehpour, A. Alabdulwahab, and A. Abusorrah, "Hourly electricity demand response in the stochastic day-ahead scheduling of coordinated electricity and natural gas networks," *IEEE Trans. Power Syst.*, vol. 31, no. 1, pp. 592–601, Jan. 2016.
[50] F. Brahman, M. Honarmand, and S. Jadid, "Optimal electrical and thermal energy management of a residential energy hub, integrating demand response and energy storage system," *Energy Buildings*, vol. 90, pp. 65–75, Mar. 2015.
[51] M. Tasdighi, H. Ghasemi, and A. Rahimi-Kian, "Residential microgrid scheduling based on smart meters data and temperature dependent thermal load modeling," *IEEE Trans. Smart Grid*, vol. 5, no. 1, pp. 349–357, Jan. 2014.
[52] E. Nabil, "A modified flower pollination algorithm for global optimization," *Expert Syst. Appl.*, vol. 57, pp. 192–203, Sep. 2016.
[53] S. M. Nigdeli, G. Bekdaş, and X.-S. Yang, "Application of the flower pollination algorithm in structural engineering," in *Metaheuristics and Optimization in Civil Engineering*. Cham, Switzerland: Springer, 2016, pp. 25–42.
[54] S. Mirjalili, A. H. Gandomi, S. Z. Mirjalili, S. Saremi, H. Faris, and S. M. Mirjalili, "Salp Swarm algorithm: A bio-inspired optimizer for engineering design problems," *Adv. Eng. Softw.*, vol. 114, pp. 163–191, Dec. 2017.
[55] S. Saremi, S. Mirjalili, and A. Lewis, "Grasshopper optimisation algorithm: Theory and application," *Adv. Eng. Softw.*, vol. 105, pp. 30–47, Mar. 2017.
[56] X. Blasco, G. Reynoso-Meza, E. A. Sánchez-Pérez, and J. V. Sánchez-Pérez, "Computing optimal distances to Pareto sets of multi-objective optimization problems in asymmetric normed lattices," *Acta Applicandae Mathematicae*, vol. 159, no. 1, pp. 75–93, Feb. 2019.

SAQIB ALI received the B.Sc. degree in electronics engineering from the University of Engineering and Technology, Taxila, and the M.Sc. degree in electrical from the University of Central Punjab, Lahore. He is currently pursuing the Ph.D. degree from the University of Engineering and Technology, Taxila, Pakistan. His area of interests include power system operation, energy management systems, and smart (mini) grid.

TAHIR NADEEM MALIK received the B.Sc. and M.Sc. degrees in electrical engineering from the University of Engineering and Technology, Lahore, and the Ph.D. degree in electrical engineering from the University of Engineering and Technology, Taxila, in 2009. His research interests include power system operation, unit commitment, economic dispatch, smart energy, machine modeling, and optimization techniques in power systems.

AAMIR RAZA received the B.Sc., M.Sc., and Ph.D. degrees in electrical engineering from the University of Engineering and Technology, Taxila, in 2004, 2010, and 2019, respectively. He is currently working as the Additional Deputy Manager of the Grid System Operations Department, Islamabad Electric Supply Company. His research interests include power system operation, smart (mini) grid, and energy hub modeling.